

DOI: 10.16108/j.issn1006-7493.2024009

引用格式: 卫炜, 隋佩珊, 陈婷婷, 黄方. 2024. 新元古代氧化事件驱动海洋Ba循环变化[J]. 高校地质学报, 30(3): 288–296

新元古代氧化事件驱动海洋 Ba 循环变化

卫 炜^{1*}, 隋佩珊¹, 陈婷婷¹, 黄 方^{1,2}

1. 中国科学技术大学 地球和空间科学学院, 中国科学院壳幔物质与环境重点实验室, 合肥 230026;

2. 中国科学技术大学 中国科学院比较行星学卓越研究中心, 合肥 230026

摘要: 新元古代晚期出现大气和海洋氧气含量显著升高的现象, 即新元古代氧化事件 (NOE)。该事件可能促使了后生动物的出现与辐射以及复杂生态系统的建立。海洋中的氧化过程可改变海水的化学组成, 如Fe、C、S的价态和种型, 而海水中Ba的生物地球化学循环则主要受S的种型及浓度的控制, 特别是硫酸根浓度。文章介绍了NOE如何改变海洋Ba循环: (1) NOE之前, 海水硫酸根浓度极低, Ba循环处于保守状态; (2) NOE期间, 海水硫酸根浓度升高, 处于重晶石过饱和状态, 导致沉积物中过剩Ba的富集以及层状重晶石的形成; (3) NOE之后, 海洋重晶石过饱和状态一直持续到古生代末期, 而中生代以后海洋硫酸根充足, Ba循环主要受控于生产力, 呈现非保守性。此外, 文章还指出, Ba同位素在重建新元古代晚期海洋Ba浓度, 继而反演海水硫酸根浓度 (即氧化程度) 研究中均具有独特的优势。

关键词: 海洋氧化; O-Fe-C-S-Ba循环; 保守元素; Ba同位素; 早期生命

中图分类号: TU991.28

文献标识码: A

文章编号: 1006-7493 (2024) 03-288-09

Changes in Oceanic Ba Cycle Driven by the Neoproterozoic Oxygenation Event

WEI Wei^{1*}, SUI Peishan¹, CHEN Tingting¹, HUANG Fang^{1,2}

1. CAS Key Laboratory of Crust-Mantle Materials and Environments, School of Earth and Space Sciences, University of Science and Technology of China, Hefei 230026, China;

2. CAS Center for Excellence in Comparative Planetology, University of Science and Technology of China, Hefei 230026, China

Abstract: The late Neoproterozoic witnessed an increase in the atmospheric and oceanic oxygen levels, namely the Neoproterozoic Oxygenation Event (NOE), likely resulting in the naissance and radiation of metazoans and the establishment of complex ecosystem. Oceanic oxygenation could change oceanic chemistry, such as species and valence states of Fe, C, and S, and the biogeochemical cycle of Ba in the ocean is strongly controlled by the S species and sulfate concentration. This review introduces how the NOE changed the oceanic Ba cycle: (1) Before the NOE, the oceanic sulfate concentration was low and the oceanic Ba cycle was conservative; (2) during the NOE, the oceanic sulfate increase led to excess Ba enrichments in sediments and formation of massive barite deposits; and (3) after the NOE, the ocean kept over-saturated relative to barite until the terminal Paleozoic and the Ba cycle was controlled by biological productivity afterwards. In addition, this review suggests to use Ba isotope system to reconstruct the oceanic Ba concentration, and indirectly to estimate the oceanic sulfate concentration (oxygenation extent) during the late Neoproterozoic.

收稿日期: 2024-01-30; 修回日期: 2024-04-23

基金项目: 国家重点研发计划 (2021YFA0718200) 资助

作者简介: 卫炜, 男, 1991年生, 副研究员, 地球化学专业; E-mail: wwei1@ustc.edu.cn

Key words: oceanic oxygenation; O-Fe-C-S-Ba cycle; conservative element; Ba isotopes; early life

Corresponding author: WEI Wei, Associate Research Professor; E-mail: wwei1@ustc.edu.cn

1 引言

地球表生系统在新元古代晚期 (800~539 Ma) 经历了一系列重大变化, 包括 Rodinia 超大陆裂解引起的海陆格局改变 (Eyles, 2008; Li et al., 2008), 以 Sturtian 和 Marinoan 冰期为代表的“雪球地球”事件和冰期之后的气温快速回暖 (Hoffman et al., 1998, 2017; Kopp et al., 2005), 以及大气与海洋氧气含量的显著提升 (新元古代氧化事件; Canfield et al., 2007; Frei et al., 2009; Lyons et al., 2014; Och and Shields-Zhou, 2011)。氧气是驱动几乎所有多细胞生物新陈代谢、生长和进化必不可少的物质, 亦有助于大型动物的复杂生命活动, 如掘穴、捕食等 (Lenton et al., 2014; Nursall, 1959)。因此, 学界普遍认为, 新元古代晚期大气和海洋的氧化导致了多细胞真核生物群的繁盛 (Brocks et al., 2017; Xiao et al., 2004) 以及后生动物的出现 (Yin et al., 2007, 2015; Yuan et al., 2011) 与多幕式辐射 (朱茂炎等, 2019; Shu et al., 2014)。

海洋中的氧化实际上是光合作用释放的氧气不断氧化海洋中还原性物质的过程, 其氧化还原状态主要受控于水体中氧化剂 (电子受体: O_2 、 NO_3^- 、 Mn^{4+} 、 Fe^{3+} 、 SO_4^{2-} 、 CH_2O) 和还原剂 (电子供体: N_2 、 Mn^{2+} 、 Fe^{2+} 、 HS^- 、 CH_2O) 之间的供给关系。因此, 新元古代氧化事件会显著改变海水的化学组成, 尤其是 Fe、S、C 等重要元素的价态和种型 (李超等, 2015; Canfield and Thamdrup, 2009; Li et al., 2010,

2020)。如表 1 所示, 海洋中不同氧化剂在氧化等量有机质的过程会释放不同程度的能量 (Libes, 2009): O_2 (有氧呼吸作用) > NO_3^- (反硝化作用) > Mn^{4+} (锰还原作用) > Fe^{3+} (铁还原作用) > SO_4^{2-} (硫酸盐还原作用) > CH_2O (产甲烷作用)。由于前一级氧化剂的存在会抑制后一级氧化剂的还原, 在有机质充足的情况下, 各类氧化剂会按上述顺序依次发挥作用 (李超等, 2015; Canfield and Thamdrup, 2009)。然而, 新元古代晚期海洋中 O_2 、 NO_3^- 、 Mn^{4+} 和 Fe^{3+} 等氧化剂处于较低水平, 因此 SO_4^{2-} 是氧化有机质的主要物质 (李超等, 2015)。 SO_4^{2-} 通过微生物硫酸盐还原作用氧化有机质, 生成 CO_2 和 HS^- (表 1); HS^- 又与水体中的 Fe^{2+} 反应生成黄铁矿沉淀 ($2HS^- + Fe^{2+} \rightarrow FeS_2 + H_2$)。当局部水体中 SO_4^{2-} 的输入通量高于 Fe^{2+} 通量两倍以上, 且有机质通量高于 Fe^{2+} 通量四倍以上时, 水体将处于缺氧硫化状态; 否则, 水体将处于缺氧富铁状态。

重晶石 ($BaSO_4$) 是一种常见的富 Ba 矿物, 其化学性质稳定, 极难溶于水, 是海洋中 Ba 最主要的汇 (Paytan and Kastner, 1996; Schoepfer et al., 2015)。重晶石的沉淀受控于水体中 Ba^{2+} 和 SO_4^{2-} 的浓度, 即其乘积相对于重晶石溶度积的高低。现代海洋中, 硫酸根充足, Ba 的浓度较低, 水体总体处于重晶石不饱和状态; 有机体死亡分解会释放大量 Ba^{2+} 进入水体, 导致重晶石过饱和微环境的形成和生物重晶石的析出, 因此 Ba 的生物地球化学循环主要受到生产力的控制, 呈现非保守性

表1 海洋中主要氧化剂消耗有机质 (1 mol CH_2O) 所释放的能量 (改自李超等, 2015)

Table 1 Energy yields from the oxidation of 1 mol CH_2O by various oceanic oxidants

氧化剂	氧化反应	反应式	释放的能量/ (kcal)
O_2	有氧呼吸	$CH_2O + O_2 \rightarrow CO_2 + H_2O$	119.6
NO_3^-	反硝化作用	$CH_2O + 4/5 NO_3^- + 4/5 H^+ \rightarrow 2/5 N_2 + 7/5 H_2O + CO_2$	113.6
Mn^{4+}	锰还原作用	$CH_2O + 2 MnO_2 + 4 H^+ \rightarrow 2 Mn^{2+} + CO_2 + 3 H_2O$	98.4
Fe^{3+}	铁还原作用	$CH_2O + 4 Fe(OH)_3 + 8 H^+ \rightarrow 4 Fe^{2+} + CO_2 + 11 H_2O$	50.4
SO_4^{2-}	硫酸盐还原作用	$CH_2O + 1/2 SO_4^{2-} + 1/2 H^+ \rightarrow 1/2 HS^- + CO_2 + H_2O$	24.4
CH_2O	产甲烷作用	$CH_2O \rightarrow 1/2 CO_2 + 1/2 CH_4$	22.4

(Bishop, 1988; Dymond et al., 1992; Ganeshram et al., 2003; Paytan and Griffith, 2007)。然而, 在新元古代氧化事件之前, 海洋硫酸根浓度长时间处于较低水平 (Algeo et al., 2015; Canfield, 1998; Fakhraee et al., 2019), 其与 Ba 浓度的乘积一直低于重晶石的溶度积, 导致 Ba 的循环可能一直处于保守状态 (Crockford et al., 2019; Wei et al., 2021a, b)。据此, 我们推测新元古代氧化事件在改变海洋氧化还原状态及化学组成的同时, 也会显著改变 Ba 的生物地球化学循环 (图 1)。本文总结了现代地表环境下 Ba 的生物地球化学循环, 介绍了新元古代氧化事件如何改变海洋的 Ba 循环, 并指出 Ba 同位素在重建新元古代晚期海洋的 Ba 浓度, 继而反演海水硫酸根浓度 (氧化程度) 方面具有独特的优势 (章节 4)。

2 现代地表环境下 Ba 的生物地球化学循环

在陆地岩石或土壤中, Ba 主要以类质同象 (替代 K) 的形式赋存于长石和云母以及富 Ba 矿物 (如重晶石、毒重石等) 中。化学风化作用可以将陆地上固态的 Ba 释放到河流 (Gong et al., 2019, 2020), 继而运移输送到海洋中 (Gou et al., 2020)。河流输送是海洋 Ba 最主要的来源, 其通量约为 6.3~8.2 Gmol/年 (Mayfield et al., 2021; Wei et al., 2021b)。

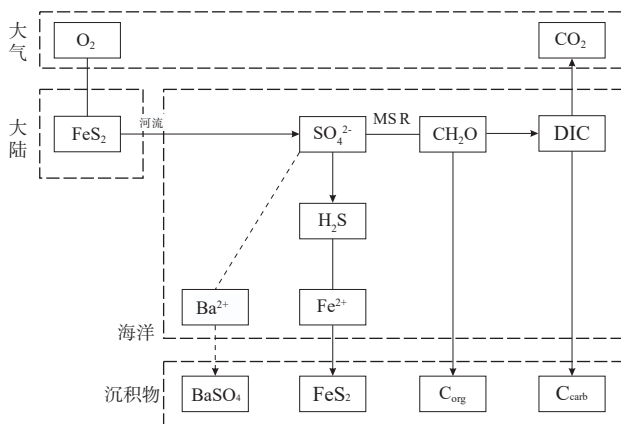


图1 新元古代晚期海洋O-S-C-Fe-Ba循环示意图 (实线连接反应物; 箭头连接反应物和生成物; 虚线表明该反应只发生在硫酸根过量的情况下; MSR: 微生物硫酸盐还原作用)

Fig. 1 Schematic diagram illustrating the O-S-C-Fe-Ba cycle in the late Neoproterozoic ocean (The solid lines connecting reactants; the arrow lines connecting reactants and products; the dashed lines representing the reaction happening when the sulfate was excessive; MSR: microbial sulfate reduction)

此外, 地下水和洋中脊热液也会为海洋提供大量的 Ba 源, 通量分别为 0.4~3.6 Gmol/年 (Mayfield et al., 2021) 和 4.6±2.2 Gmol/年 (Zhang et al., 2024)。

在现代海洋中, Ba 的浓度 ([Ba]) 呈类营养元素分布趋势。以大西洋 18 站点 (阿根廷盆地) 为例: [Ba] 在表层水体 (深度小于 100 米) 较低 (41.7~45.8 nM), 随着水深增加而逐渐升高至 106.9 nM (图 2a; Bridgestock et al., 2018)。现代海洋的硫酸根充足 (平均值为 28 mM; Algeo et al., 2015), 由于 Ba 浓度较低, 总体上处于重晶石不饱和环境 (Monnin et al., 1999)。但是, 表层水体中的初级生产者在死亡分解时会释放大量的 Ba 进入到水体中; 无定型的富 P 组分首先与 Ba 结合, 随后被硫酸根替代, 形成重晶石过饱和微环境 (Martinez-Ruiz et al., 2018, 2019), 促使生物重晶石颗粒 (粒径小于 5 μm, 常呈自形的椭圆体; Paytan et al., 2002) 的沉淀。在深部水体或水岩界面附近, 生物重晶石在沉降过程中, 会由于水体的重晶石不饱和再次溶解, 释放部分 Ba 回到水体中 (Falkner et al., 1993; Monnin et al., 1999)。

在沉积物中, 有机质会按 O₂、NO₃⁻、Mn⁴⁺、Fe³⁺、SO₄²⁻ 的顺序依次消耗孔隙水中的氧化剂 (表 1; Canfield and Thamdrup, 2009; Schunck et al., 2013)。在硫酸盐—甲烷转换带以下, 孔隙水中的硫酸根由于微生物硫酸盐还原作用消耗殆尽, 继而导致生物重晶石再次溶解 (Dickens et al., 2003; Snyder et al., 2007; Torres et al., 1996)。尽管如此, 由于生物重晶石的形成与表层水体的生产力水平紧密相关, 许多大陆边缘和开阔大洋海域中沉积物中生物重晶石和有机质沉降通量仍呈现出良好的线性正相关关系 (Carter et al., 2020; Dymond et al., 1992; Fagel et al., 2004; McManus et al., 2002; Sternberg et al., 2007; Sun et al., 2013)。因此, 沉积物中生物重晶石或过剩 (非碎屑组分) Ba 的累积速率经常用来反映不同地区或时期的输出生产力水平 (Carter et al., 2016; Dymond et al., 1992; Eagle et al., 2003; Klump et al., 2001; Ma et al., 2015; Paytan and Kastner, 1996)。

3 新元古代氧化事件驱动海洋 Ba 循环变化

在新元古代氧化事件之前, 大气中的氧气含

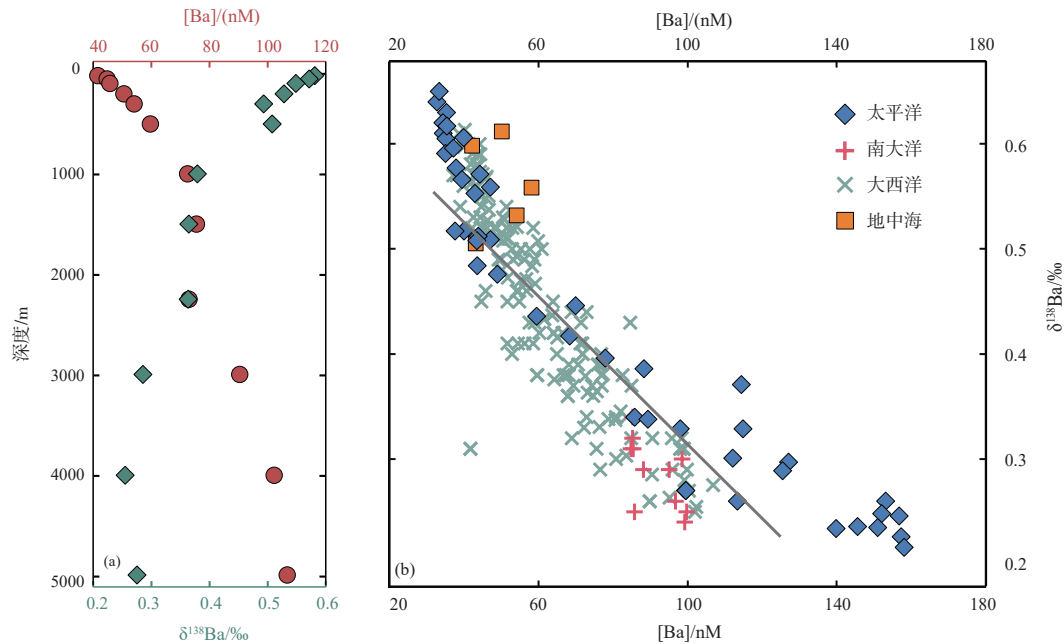


图2 (a) 大西洋18站点(阿根廷盆地)海水[Ba]和 $\delta^{138}\text{Ba}$ 值随深度变化图(Bridgestock et al., 2018); (b) 海水[Ba]和 $\delta^{138}\text{Ba}$ 相关性图解(Bates et al., 2017; Bridgestock et al., 2018; Cao et al., 2020; Geyman et al., 2019; Hemsing et al., 2018; Horner et al., 2015;

Hsieh and Henderson, 2017; Pretet et al., 2015)

Fig. 2 (a) Seawater depth profiles of dissolved Ba concentrations and $\delta^{138}\text{Ba}$ values at the Station 18 of the Atlantic Ocean (Argentine Basin) (Bridgestock et al., 2018); (b) Cross-plot of Ba concentrations versus $\delta^{138}\text{Ba}$ values of the modern seawater (Bates et al., 2017; Bridgestock et al., 2018; Cao et al., 2020; Geyman et al., 2019; Hemsing et al., 2018; Horner et al., 2015; Hsieh and Henderson, 2017; Pretet et al., 2015)

量较低(低于现代水平的1%; Cole et al., 2016; Planavsky et al., 2014), 河流、地下水、海洋等地表环境也处于高度的还原状态(硫酸根浓度低)。因此, 河流、地下水以及洋中脊热液向海洋输送的Ba通量应远远高于现代水平(Gou et al., 2020; Mayfield et al., 2021; Zhang et al., 2024)。现代海洋中的Ba主要是被生物重晶石移除, 碳酸盐岩和铁锰氧化物也可移除小部分的Ba, 但其通量较小(Dymond et al., 1992; Eagle et al., 2003; Gonneea and Paytan, 2006; Schoepfer et al., 2015)。但是, 在新元古代氧化事件之前的还原性海洋中, 极低的硫酸根浓度(<0.4 mM; Algeo et al., 2015; Canfield, 1998; Fakhraee et al., 2019)导致其与Ba浓度的乘积低于重晶石的溶度积, 因此重晶石无法大量形成, 即Ba无法被移除。在此情况下, 河流、地下水、洋中脊热液输入的Ba不断在海洋中积累, 但仍未达到可以析出重晶石的水平。即使表层氧化水体中会有些许生物重晶石形成, 也会很快在深部缺氧水体中再次溶解(Falkner et al., 1993; Wei et al., 2021b)。据此推测, 新元古代氧化事件之前的海洋中存在一个巨大的、均一的Ba库(Crockford et

al., 2019; Wei et al., 2021a, 2021b), 其Ba浓度可能高于18.6 μM (Wei et al., 2021a)。由于该时期海洋硫酸根储库受限, 整体处于重晶石不饱和状态, 因此沉积物中的过剩Ba含量总体处于较低水平(图3; Wei et al., 2021a)。层状重晶石矿床在此期间也没有大规模形成, 只在太古宙(澳大利亚西部、南非和印度)和中元古代(印度和南非)零星出现(Han et al., 2022; Jewell, 2000): 前者可能与蒸发作用、变质作用以及成岩作用有关, 较低的硫酸根硫同位素值(2.0‰~5.4‰)表明其形成与海水硫酸根浓度升高无关(Jewell, 2000); 后者的硫酸根硫同位素值较高(20.2‰~45.5‰), 表明其形成与局部水体的硫酸根浓度略微提升有关(George et al., 2013; McClung et al., 2007)。

随着新元古代晚期大气开始氧化, 陆地氧化风化作用增强, 河流输送大量硫酸根进入海洋, 导致海洋硫酸根浓度升高(<2 mM; Loyd et al., 2012; Osburn et al., 2015)。在现代海洋沉积物中, 硫酸盐—甲烷转换带之上孔隙水硫酸根浓度因微生物还原作用不断降低, 但重晶石由于孔隙水中硫酸根的存在保持稳定; 在硫酸盐—甲烷转换带以下, 孔隙

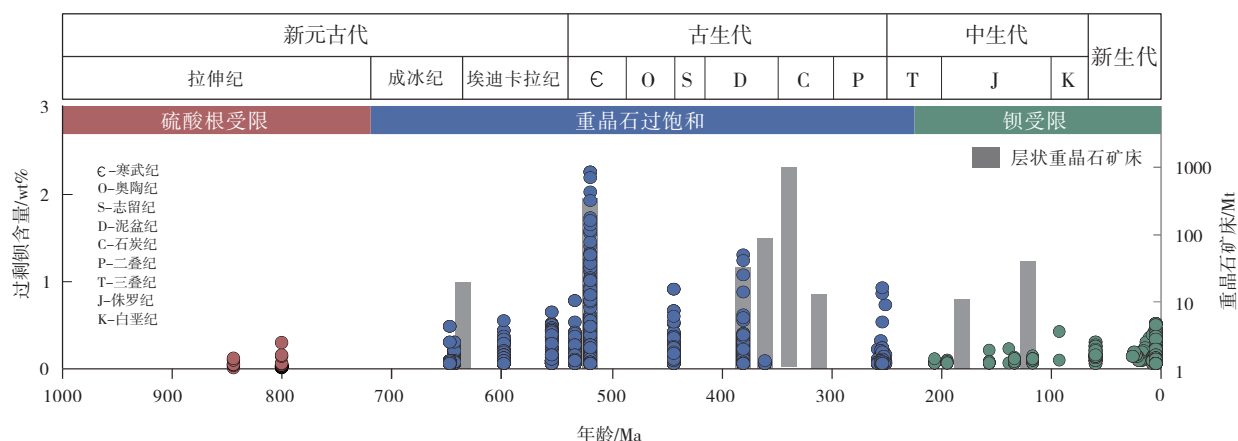


图3 新元古代以来沉积物中过剩Ba含量和层状重晶石矿床产量变化趋势(改编自Wei et al., 2021a和Han et al., 2022)

Fig. 3 Temporal trends in Ba excess contents in sediments and sizes of massive barite deposits from the Neoproterozoic to the present (modified after Wei et al., 2021a and Han et al., 2022)

水中硫酸根耗尽,重晶石开始溶解(Henkel et al., 2012; Riedinger et al., 2006)。据此,我们推测新元古代晚期海洋中硫酸根将优先与有机质通过微生物硫酸盐还原作用生成 H_2S ; H_2S 又与溶解的 Fe^{2+} 反应生成黄铁矿沉淀;当硫酸根过量时,则会与水体中的Ba反应生成重晶石。随着离岸距离的增加,硫酸根和有机质不断被消耗,因此局部水体的氧化还原状态及重晶石饱和状态受 SO_4^{2-} 、 CH_2O 和 Fe^{2+} 的输入通量控制:(1)当 $2SO_4^{2-} > CH_2O > 4Fe^{2+}$ 时,有黄铁矿生成, H_2S 残余导致水体硫化,同时 SO_4^{2-} 残余导致重晶石沉淀;(2)当 $CH_2O > 2SO_4^{2-} > 4Fe^{2+}$ 时,水体硫化,但 SO_4^{2-} 消耗殆尽,无重晶石沉淀;(3)当 $2SO_4^{2-} > 4Fe^{2+} > CH_2O$ 时,有黄铁矿生成, H_2S 消耗殆尽,水体铁化,有重晶石沉淀;(4)当 $CH_2O > 4Fe^{2+} > 2SO_4^{2-}$ 时,水体铁化,无重晶石沉淀;(5)当 $4Fe^{2+} > CH_2O > 2SO_4^{2-}$ 或 $4Fe^{2+} > 2SO_4^{2-} > CH_2O$ 时,水体铁化,虽仍有黄铁矿和(或)重晶石形成,但有机质和硫酸根已被消耗到很低水平,因此两者沉积通量较小。由此可见,新元古代晚期海洋中局部水体重晶石的沉淀主要受控与有机质和硫酸根的输入通量,当 $2SO_4^{2-} > CH_2O$ 时,会发生重晶石沉淀。从全球尺度来看,随着新元古代晚期海洋的逐渐氧化(Canfield et al., 2007; Chen et al., 2015; Wei et al., 2023)和硫酸根浓度的升高(Algeo et al., 2015; Shi et al., 2022),海洋处于重晶石过饱和环境,此前巨大的均一Ba储库不断被消除,致使该时期沉积物中过剩Ba的富集(图3; Wei et al., 2021a),以

及一些层状重晶石的形成,尤其是在全球范围广泛出现的沉积于“雪球地球”事件之后的盖帽碳酸盐岩地层中(Crockford et al., 2019; Han et al., 2022; Jewell, 2000)。

在新元古代氧化事件之后,大气和海洋已显著氧化(Chen et al., 2015; Lyons et al., 2014; Planavsky et al., 2014; Wei et al., 2023),但总体氧化程度仍低于现代水平(Algeo et al., 2015),存在许多区域性的还原水体,其中含有大量的还原性物质(如 Fe^{2+} 、 H_2S 、 CH_2O 等)和 Ba^{2+} 。区域内硫酸根浓度的突增会使水体达到重晶石过饱和状态,致使古生代(539~252 Ma)沉积物中过剩Ba的富集和层状重晶石矿床的形成(图3; Han et al., 2022; Jewell, 2000; Wei et al., 2021a)。在此之后(中生代和新生代),沉积物中的过剩Ba含量明显降低,层状重晶石矿消失(图3),表明海洋中Ba的生物地球化学循环可能与现代海洋类似,受到生产力的控制,呈非保守性(Wei et al., 2021a)。

4 Ba同位素示踪海洋中Ba的生物地球化学循环

Ba同位素是新近发展的金属稳定同位素体系,已广泛用于示踪海洋中Ba的生物地球化学循环(Bridgestock et al., 2019; Crockford et al., 2019; Hodgskiss et al., 2019; Wei et al., 2021b; Zhang et al., 2022)。Ba有七个稳定同位素, ^{130}Ba 、 ^{132}Ba 、 ^{134}Ba 、 ^{135}Ba 、 ^{136}Ba 、 ^{137}Ba 和 ^{138}Ba ,在自然界的丰度分别

为 0.11‰、0.10‰、2.42‰、6.59‰、7.85‰、11.23‰ 和 71.70‰。学界通常以 $\delta^{138}\text{Ba} = [(^{138}\text{Ba}/^{134}\text{Ba})_{\text{样品}} / (^{138}\text{Ba}/^{134}\text{Ba})_{\text{SRM3104a}} - 1] \times 1000 (\text{‰})$ 表示样品的 Ba 同位素组成。

上地壳的平均 $\delta^{138}\text{Ba}$ 值为 $0.00 \pm 0.04 \text{‰}$ (Nan et al., 2018)。风化过程会优先释放陆壳中偏重的 Ba 同位素 (Gong et al., 2019)，导致河水的 Ba 同位素组成偏重 (平均值为 0.17‰ ; Cao et al., 2020; Gou et al., 2020; Wei et al., 2021b)。此外，地下水和洋中脊热液的平均 $\delta^{138}\text{Ba}$ 值分别为 $0.00 \pm 0.04 \text{‰}$ (Mayfield et al., 2021) 和 $-0.17 \text{‰} \pm 0.05 \text{‰}$ (Zhang et al., 2024)。现代海洋中海水 $\delta^{138}\text{Ba}$ 值随深度的变化趋势与 [Ba] 相反。例如，大西洋 18 站点 (阿根廷盆地) 海水的 $\delta^{138}\text{Ba}$ 值在表层水体 (深度小于 100 米) 较高 (0.55‰ 至 0.58‰)，随着水深增加而逐渐降低至 0.25‰ (图 2a; Bridgestock et al., 2018)。这是由于生物重晶石在形成过程中会优先利用水体中偏轻的 Ba 同位素 (Bates et al., 2017; Bridgestock et al., 2018; Horner et al., 2015; Hsieh and Henderson, 2017)，而在深部水体中重晶石溶解过程将轻 Ba 同位素重新释放回水体中 (该过程不会发生明显的 Ba 同位素分馏; Bridgestock et al., 2018, 2019; Horner et al., 2017)。此外，大洋环流也会重新分布海水的 [Ba] 和 $\delta^{138}\text{Ba}$ 值，导致两者之间呈现出良好的线性负相关关系 (图 2b; Bates et al., 2017; Cao et al., 2020; Horner et al., 2015; Hsieh and Henderson, 2017)。根据该相关性，可推算出生物重晶石形成过程的 Ba 同位素分馏 ($\Delta_{\text{颗粒态-溶解态}}$) 在 -0.52‰ 和 -0.35‰ 之间 (Bates et al., 2017; Bridgestock et al., 2018; Horner et al., 2015; Hsieh and Henderson, 2017)。该结果与实验测定的重晶石形成过程的 Ba 同位素分馏 (-0.35‰ 至 -0.25‰ ; Böttcher et al., 2018; von Allmen et al., 2010) 以及现代低硫酸根浓度湖水中发现的生物重晶石形成过程的 Ba 同位素分馏 ($-0.41 \text{‰} \pm 0.09 \text{‰}$; Horner et al., 2017) 接近。因此，沉积物中过剩 Ba 的同位素组成可以用于反演其沉积环境的输出生产力水平 (Bridgestock et al., 2018, 2019)。相比于过剩 Ba 的累积速率，过剩 Ba 同位素组成不会受到沉积物中其他组分 (如碳酸盐; Torfstein et al., 2010) 以及重晶石保存率 (Dickens et al., 2003) 的干扰。

如上所述，新元古代氧化事件之前的海洋中存在一个巨大的、均一的 Ba 库 (Crockford et al., 2019; Wei et al., 2021a, 2021b)。由于河流 (0.17‰ ; Cao et al., 2020; Gou et al., 2020; Wei et al., 2021b)、地下水 ($0.00 \text{‰} \pm 0.04 \text{‰}$; Mayfield et al., 2021)、洋中脊热液 ($-0.17 \text{‰} \pm 0.05 \text{‰}$; Zhang et al., 2024) 以及现代生物重晶石 ($0.04 \text{‰} \pm 0.13 \text{‰}$; Crockford et al., 2019) 的 $\delta^{138}\text{Ba}$ 值相较于现代海洋 (0.17‰ 至 0.65‰ ; 图 2b) 明显偏低，我们推测新元古代之前海水中的 Ba 库相比现代海水是偏轻的 (Crockford et al., 2019; Wei et al., 2021b)。当大气和海洋的氧气含量逐渐上升，海水硫酸根浓度提高时，重晶石开始形成并沉淀。该过程也是优先利用水体中偏轻的 Ba 同位素 (von Allmen et al., 2010; Wang et al., 2021)，致使海水的 $\delta^{138}\text{Ba}$ 值不断升高。我们可根据下列公式计算出新元古代氧化事件期间海水的平均 Ba 浓度：

$$R + F_{\text{out}} = R_0 \quad (1)$$

$$R \times \delta_{\text{sw}} + F_{\text{out}} \times \delta_{\text{out}} = R_0 \times \delta_{\text{sw0}} \quad (2)$$

$$R/R_0 = (\delta_{\text{sw0}} - \delta_{\text{out}}) / (\delta_{\text{sw}} - \delta_{\text{out}}) = (\delta_{\text{sw0}} - \delta_{\text{out}}) / \Delta_{\text{barite}} \quad (3)$$

$$m_{\text{Ba}} = m_{\text{Ba0}} \times (R/R_0) \quad (4)$$

其中， R_0 和 R 是新元古代氧化事件之前和期间的 Ba 库大小， F_{out} 是被硫酸根移除的 Ba 通量， δ_{sw0} 和 δ_{sw} 分别是新元古代氧化事件之前 (-0.2‰ ; Wei et al., 2021b) 和期间 Ba 库的 $\delta^{138}\text{Ba}$ 值， δ_{out} 是沉积物中过剩 Ba 的 $\delta^{138}\text{Ba}$ 值， m_{Ba0} 和 m_{Ba} 分别是新元古代氧化事件之前 (18.6 μM ; Wei et al., 2021a) 和期间海水的平均 Ba 浓度， Δ_{barite} 是海水与沉积物之间的 Ba 同位素平衡分馏 (0.23‰ ; Wang et al., 2021)。由于新元古代氧化事件期间海水处于重晶石过饱和和环境，我们又可借助公式 (1~4) 计算出的平均 Ba 浓度以及下列公式得到当时海水的平均硫酸根浓度：

$$\text{Kd}(T, P) = (\gamma_{\text{Ba}} \times f_{\text{Ba}} \times m_{\text{Ba}}) \times (\gamma_{\text{SO}_4} \times f_{\text{SO}_4} \times m_{\text{SO}_4}) \quad (5)$$

其中， Kd 是热力学溶度积， γ 是简单活度系数， f 是游离离子占比， m 是浓度。假设新元古代晚期海洋温度 (25℃) 和气压 (一个标准大气压) 与现代海洋接近，可将 Kd 、 γ_{Ba} 、 f_{Ba} 、 γ_{SO_4} 和 f_{SO_4} 值分别设为 1.1×10^{-10} 、0.24、0.93、0.17 和 0.39 (Church and Wolgemuth, 1972)。据此，可以根据新元古代晚期沉积物中过剩 Ba 的 $\delta^{138}\text{Ba}$ 值推算出其沉积时期海

水的平均Ba浓度,继而反演海水的平均硫酸根浓度,即氧化程度。

5 总结与展望

地质历史上,海洋Ba的生物地球化学循环经历了显著的变化。新元古代氧化事件之前,海洋硫酸根浓度极低,长期处于重晶石不饱和状态,因此Ba在海洋中不断积累,形成一个巨大且均一的库,呈现保守特征。新元古代氧化事件期间,海洋硫酸根浓度升高,处于重晶石过饱和状态,导致沉积物中过剩Ba的富集以及层状重晶石的形成。在此之后,海洋重晶石过饱和状态一直持续到古生代末期;中生代之后,海洋硫酸根充足,Ba的循环主要受控于生产力水平,呈现非保守性。Ba同位素是新近的古海洋指标,在重建新元古代晚期海洋Ba浓度,继而反演海水硫酸根浓度(即氧化程度)方面具有独特的优势。

参考文献 (References):

- 李超,程猛,Algeo T J,等. 2015. 早期地球海洋水化学分带的理论预测[J]. 中国科学: 地球科学, 45: 1829–1838.
- 朱茂炎,赵方臣,殷宗军,等. 2019. 中国的寒武纪大爆发研究: 进展与展望[J]. 中国科学: 地球科学, 49(10): 1455–1490.
- Algeo T, Luo G, Song H, et al. 2015. Reconstruction of secular variation in seawater sulfate concentrations [J]. *Biogeosciences*, 12(7): 2131–2151.
- Bates S L, Hendry K R, Pryer H V, et al. 2017. Barium isotopes reveal role of ocean circulation on barium cycling in the Atlantic [J]. *Geochimica et Cosmochimica Acta*, 204: 286–299.
- Bishop J K. 1988. The barite–opal–organic carbon association in oceanic particulate matter [J]. *Nature*, 332: 341–343.
- Bridgestock L, Hsieh Y T, Porcelli D, et al. 2018. Controls on the barium isotope compositions of marine sediments [J]. *Earth and Planetary Science Letters*, 481: 101–110.
- Bridgestock L, Hsieh Y T, Porcelli D, et al. 2019. Increased export production during recovery from the Paleocene–Eocene thermal maximum constrained by sedimentary Ba isotopes [J]. *Earth and Planetary Science Letters*, 510: 53–63.
- Brocks J J, Jarrett A J M, Sirantoine E, et al. 2017. The rise of algae in Cryogenian oceans and the emergence of animals [J]. *Nature*, 548(7669): 578–581.
- Böttcher M E, Neubert N, von Allmen K, et al. 2018. Barium isotope fractionation during the experimental transformation of aragonite to witherite and of gypsum to barite, and the effect of ion (de)solvation [J]. *Isotopes in Environmental and Health Studies*, 54(3): 324–335.
- Canfield D E. 1998. A new model for Proterozoic ocean chemistry [J]. *Nature*, 396: 450–453.
- Canfield D E, Poulton S W and Narbonne G M. 2007. Late-Neoproterozoic deep-ocean oxygenation and the rise of animal life [J]. *Science*, 315(5808): 92–95.
- Canfield D E and Thamdrup B. 2009. Towards a consistent classification scheme for geochemical environments, or, why we wish the term “suboxic” would go away [J]. *Geobiology*, 7(4): 385–392.
- Cao Z, Siebert C, Hathorne E C, et al. 2020. Corrigendum to “Constraining the oceanic barium cycle with stable barium isotopes” [Earth Planet. Sci. Lett. 434 (2016) 1–9] [J]. *Earth and Planetary Science Letters*, 530: 116003.
- Carter S C, Griffith E M and Penman D E. 2016. Peak intervals of equatorial Pacific export production during the middle Miocene climate transition [J]. *Geology*, 44(11): 923–926.
- Carter S C, Paytan A and Griffith E M. 2020. Toward an improved understanding of the marine barium cycle and the application of marine barite as a paleoproductivity proxy [J]. *Minerals*, 10(5): 421.
- Chen X, Ling H F, Vance D, et al. 2015. Rise to modern levels of ocean oxygenation coincided with the Cambrian radiation of animals [J]. *Nature Communications*, 6: 7142.
- Church T M and Wolgemuth K. 1972. Marine barite saturation [J]. *Earth and Planetary Science Letters*, 15(1): 35–44.
- Cole D B, Reinhard C T, Wang X, et al. 2016. A shale-hosted Cr isotope record of low atmospheric oxygen during the Proterozoic [J]. *Geology*, 44(7): 555–558.
- Crockford P W, Wing B A, Paytan A, et al. 2019. Barium-isotopic constraints on the origin of post-Marinoan barites [J]. *Earth and Planetary Science Letters*, 519: 234–244.
- Dickens G R, Fewless T, Thomas E, et al. 2003. Excess barite accumulation during the Paleocene–Eocene thermal maximum: Massive input of dissolved barium from seafloor gas hydrate reservoirs [J]. *Geological Society America Special Paper*, 369: 11–24.
- Dymond J, Suess E and Lyle M. 1992. Barium in deep-sea sediment: A geochemical proxy for paleoproductivity [J]. *Paleoceanography*, 7(2): 163–181.
- Eagle M, Paytan A, Arrigo K R, et al. 2003. A comparison between excess barium and barite as indicators of carbon export [J]. *Paleoceanography*, 18(1): 1021.
- Eyles N. 2008. Glacio-epochs and the supercontinent cycle after ~3.0 Ga: Tectonic boundary conditions for glaciation [J]. *Palaeogeography, Palaeoclimatology, Palaeoecology*, 258(1–2): 89–129.
- Fagel N, Dehairs F, Peinert R, et al. 2004. Reconstructing export production at the NE Atlantic margin: Potential and limits of the Ba proxy [J]. *Marine Geology*, 204(1–2): 11–25.
- Fakhraee M, Hancisse O, Canfield D E, et al. 2019. Proterozoic seawater sulfate scarcity and the evolution of ocean-atmosphere chemistry [J]. *Nature Geoscience*, 12: 375–380.
- Falkner K K, Klinkhammer G P, Bowers T S, et al. 1993. The behavior of barium in anoxic marine waters [J]. *Geochimica et Cosmochimica Acta*, 57(3): 537–554.
- Frei R, Gaucher C, Poulton S W, et al. 2009. Fluctuations in Precambrian atmospheric oxygenation recorded by chromium isotopes [J]. *Nature*, 461: 250–253.
- Ganeshram R S, François R, Commeau J, et al. 2003. An experimental investigation of barite formation in seawater [J]. *Geochimica et Cosmochimica Acta*, 67(14): 2599–2605.
- George B G, Shalini N, Pandian M S, et al. 2013. Strontium and sulphur

- isotopic constraints on the formation of the Mangampeta barite deposit, Cuddapah Basin [J]. *Current Science*, 105: 499–504.
- Geyman B M, Ptacek J L, LaVigne M, et al. 2019. Barium in deep-sea bamboo corals: Phase associations, barium stable isotopes, & prospects for paleoceanography [J]. *Earth and Planetary Science Letters*, 525: 115751.
- Gong Y, Zeng Z, Cheng W, et al. 2020. Barium isotopic fractionation during strong weathering of basalt in a tropical climate [J]. *Environment International*, 143: 105896.
- Gong Y, Zeng Z, Zhou C, et al. 2019. Barium isotopic fractionation in latosol developed from strongly weathered basalt [J]. *Science of The Total Environment*, 687: 1295–1304.
- Gonneea M E and Paytan A. 2006. Phase associations of barium in marine sediments [J]. *Marine Chemistry*, 100(1–2): 124–135.
- Gou L-F, Jin Z, Galy A, et al. 2020. Seasonal riverine barium isotopic variation in the middle Yellow River: Sources and fractionation [J]. *Earth and Planetary Science Letters*, 531: 115990.
- Han T, Peng Y and Bao H. 2022. Sulfate-limited euxinic seawater facilitated Paleozoic massively bedded barite deposition [J]. *Earth and Planetary Science Letters*, 582: 117419.
- Hemsing F, Hsieh Y T, Bridgestock L, et al. 2018. Barium isotopes in cold-water corals [J]. *Earth and Planetary Science Letters*, 491: 183–192.
- Henkel S, Mogollón J M, Nöthen K, et al. 2012. Diagenetic barium cycling in Black Sea sediments—A case study for anoxic marine environments [J]. *Geochimica et Cosmochimica Acta*, 88: 88–105.
- Hodgskiss M S W, Crockford P W, Peng Y, et al. 2019. A productivity collapse to end Earth's Great Oxidation [J]. *Proceedings of the National Academy of Sciences of the United States of America*, 116(35): 17207–17212.
- Hoffman P F, Abbot D S, Ashkenazy Y, et al. 2017. Snowball Earth climate dynamics and Cryogenian geology–geobiology [J]. *Science Advances*, 3(11): e1600983.
- Hoffman P F, Kaufman A J, Halverson G P, et al. 1998. A Neoproterozoic snowball Earth. *Science*, 281(5381): 1342–1346.
- Horner T J, Kinsley C W and Nielsen S G. 2015. Barium-isotopic fractionation in seawater mediated by barite cycling and oceanic circulation [J]. *Earth and Planetary Science Letters*, 430: 511–522.
- Horner T J, Pryer H V, Nielsen S G, et al. 2017. Pelagic barite precipitation at micromolar ambient sulfate [J]. *Nature Communications*, 8: 1342.
- Hsieh Y T and Henderson G M. 2017. Barium stable isotopes in the global ocean: Tracer of Ba inputs and utilization [J]. *Earth and Planetary Science Letters*, 473: 269–278.
- Jewell P W. 2000. Bedded barite in the geologic record [C]//Glenn C R, Prévôt-Lucas L, Lucas J. *Marine authigenesis: from global to microbial*. SEPM Special Publication: 147–161.
- Klump J, Hebbeln D and Wefer G. 2001. High concentrations of biogenic barium in Pacific sediments after Termination I—A signal of changes in productivity and deep water chemistry [J]. *Marine Geology*, 177(1–2): 1–11.
- Kopp R E, Kirschvink J L, Hilburn I A, et al. 2005. The Paleoproterozoic snowball Earth: A climate disaster triggered by the evolution of oxygenic photosynthesis [J]. *Proceedings of the National Academy of Sciences of the United States of America*, 102(32): 11131–11136.
- Lenton T M, Boyle R A, Poulton S W, et al. 2014. Co-evolution of eukaryotes and ocean oxygenation in the Neoproterozoic era [J]. *Nature Geoscience*, 7: 257–265.
- Li C, Love G D, Lyons T W, et al. 2010. A stratified redox model for the Ediacaran ocean [J]. *Science*, 328(5974): 80–83.
- Li C, Shi W, Cheng M, et al. 2020. The redox structure of Ediacaran and early Cambrian oceans and its controls [J]. *Science Bulletin*, 65(24): 2141–2149.
- Libes S M. 2009. *Introduction to Marine Biogeochemistry* [M]. 2nd ed. Burlington–San Diego–London: Elsevier Academic Press.
- Li X, Bogdanova S V, Collins A S, et al. 2008. Assembly, configuration, and break-up history of Rodinia: A synthesis [J]. *Precambrian Research*, 160(1–2): 179–210.
- Lloyd S J, Marengo P J, Hagadorn J W, et al. 2012. Sustained low marine sulfate concentrations from the Neoproterozoic to the Cambrian: insights from carbonates of northwestern Mexico and eastern California [J]. *Earth and Planetary Science Letters*, 339–340: 79–94.
- Lyons T W, Reinhard C T and Planavsky N J. 2014. The rise of oxygen in Earth's early ocean and atmosphere [J]. *Nature*, 506: 307–315.
- Ma Z, Gray E, Thomas E, et al. 2014. Carbon sequestration during the Palaeocene–Eocene Thermal Maximum by an efficient biological pump [J]. *Nature Geoscience*, 7(5): 382–388.
- Martinez-Ruiz F, Jroundi F, Paytan A, et al. 2018. Barium bioaccumulation by bacterial biofilms and implications for Ba cycling and use of Ba proxies [J]. *Nature Communications*, 9: 1619.
- Martinez-Ruiz F, Paytan A, Gonzalez-Muñoz M T, et al. 2019. Barite formation in the ocean: Origin of amorphous and crystalline precipitates [J]. *Chemical Geology*, 511: 441–451.
- Mayfield K K, Eisenhauer A, Santiago Ramos D P, et al. 2021. Groundwater discharge impacts marine isotope budgets of Li, Mg, Ca, Sr, and Ba [J]. *Nature Communications*, 12: 148.
- McClung C R, Gutzmer J, Beukes N J, et al. 2007. Geochemistry of bedded barite of the Mesoproterozoic Aggenys–Gamsberg Broken Hill-type district, South Africa [J]. *Mineralium Deposita*, 42: 537–549.
- McManus J, Dymond J, Dunbar R B, et al. 2002. Particulate barium fluxes in the Ross Sea [J]. *Marine Geology*, 184(1–2): 1–15.
- Monnin C, Jeandel C, Cattalio T, et al. 1999. The marine barite saturation state of the world's oceans [J]. *Marine Chemistry*, 65(3–4): 253–261.
- Nan X-Y, Yu H-M, Rudnick R L, et al. 2018. Barium isotopic composition of the upper continental crust [J]. *Geochimica et Cosmochimica Acta*, 233: 33–49.
- Nursall J R. 1959. Oxygen as a prerequisite to the origin of the Metazoa [J]. *Nature*, 183: 1170–1172.
- Och L M and Shields-Zhou G A. 2012. The Neoproterozoic oxygenation event: Environmental perturbations and biogeochemical cycling [J]. *Earth-Science Reviews*, 110(1–4): 26–57.
- Osburn M R, Owens J, Bergmann K D, et al. 2015. Dynamic changes in sulfate sulfur isotopes preceding the Ediacaran Shuram Excursion [J]. *Geochimica et Cosmochimica Acta*, 170: 204–224.
- Paytan A and Griffith E M. 2007. Marine barite: Recorder of variations in ocean export productivity [J]. *Deep Sea Research Part II: Topical Studies in Oceanography*, 54(5–7): 687–705.
- Paytan A and Kastner M. 1996. Benthic Ba fluxes in the central Equatorial Pacific, implications for the oceanic Ba cycle [J]. *Earth and Planetary Science Letters*, 142(3–4): 439–450.
- Paytan A, Mearon S, Cobb K, et al. 2002. Origin of marine barite deposits:

- Sr and S isotope characterization [J]. *Geology*, 30(8): 747–750.
- Planavsky N J, Reinhard C T, Wang X, et al. 2014. Low Mid-Proterozoic atmospheric oxygen levels and the delayed rise of animals [J]. *Science*, 346(6209): 635–638.
- Pretet C, Zuilen K V, Nägler T F, et al. 2015. Constraints on barium isotope fractionation during aragonite precipitation by corals [J]. *The Depositional Record*, 1(2): 118–129.
- Riedinger N, Kasten S, Groger J, et al. 2006. Active and buried authigenic barite fronts in sediments from the eastern Cape Basin [J]. *Earth and Planetary Science Letters*, 241: 876–887.
- Schoepfer S D, Shen J, Wei H, et al. 2015. Total organic carbon, organic phosphorus, and biogenic barium fluxes as proxies for paleomarine productivity [J]. *Earth-Science Reviews*, 149: 23–52.
- Schunck H, Lavik G, Desai D K, et al. 2013. Giant hydrogen sulfide plume in the oxygen minimum zone off Peru supports chemolithoautotrophy [J]. *PLoS One*, 8(8): e68661.
- Shi W, Mills B J W, Li C, et al. 2022. Decoupled oxygenation of the Ediacaran ocean and atmosphere during the rise of early animals [J]. *Earth and Planetary Science Letters*, 591: 117619.
- Shu D, Isozaki Y, Zhang X, et al. 2014. Birth and early evolution of metazoans [J]. *Gondwana Research*, 25(3): 884–895.
- Snyder G, Dickens G and Castellini D. 2007. Labile barite contents and dissolved barium concentrations on Blake Ridge: New perspectives on barium cycling above gas hydrate systems [J]. *Journal of Geochemical Exploration*, 95(1–3): 48–65.
- Sternberg E, Jeandel C, Miquel J C, et al. 2007. Particulate barium fluxes and export production in the northwestern Mediterranean [J]. *Marine chemistry*, 105(3–4), 281–295.
- Sun W, Han Z, Hu C, et al. 2013. Particulate barium flux and its relationship with export production on the continental shelf of Prydz Bay, east Antarctica [J]. *Marine Chemistry*, 157: 86–92.
- Torfstein A, Winckler G and Tripathi A. 2010. Productivity feedback did not terminate the Paleocene–Eocene thermal maximum (PETM) [J]. *Climate of the Past*, 6(2): 265–272.
- Torres M, Brumsack H, Bohrmann G, et al. 1996. Barite fronts in continental margin sediments: A new look at barium remobilization in the zone of sulfate reduction and formation of heavy barites in diagenetic fronts [J]. *Chemical Geology*, 127(1–3): 125–139.
- von Allmen K, Böttcher M E, Samankassou E, et al. 2010. Barium isotope fractionation in the global barium cycle: First evidence from barium minerals and precipitation experiments [J]. *Chemical Geology*, 277(1–2): 70–77.
- Wang W, Wu Z and Huang F. 2021. Equilibrium barium isotope fractionation between minerals and aqueous solution from first-principles calculations [J]. *Geochimica et Cosmochimica Acta*, 292: 64–77.
- Wei G Y, Ling H F, Shields G A, et al. 2021a. Revisiting stepwise ocean oxygenation with authigenic barium enrichments in marine mudrocks [J]. *Geology*, 49(9): 1059–1063.
- Wei W, Chen X, Ling H F, et al. 2023. Vanadium isotope evidence for widespread marine oxygenation from the late Ediacaran to early Cambrian [J]. *Earth and Planetary Science Letters*, 602: 117942.
- Wei W, Zeng Z, Shen J, et al. 2021. Dramatic changes in the carbonate-hosted barium isotopic compositions in the Ediacaran Yangtze Platform [J]. *Geochimica et Cosmochimica Acta*, 299: 113–129.
- Xiao S H. 2004. New multicellular algal fossils and acritarchs in Doushantuo chert nodules (Neoproterozoic; Yangtze Gorges, south China) [J]. *Journal of Paleontology*, 78(2): 393–401.
- Yin L, Zhu M, Knoll A H, et al. 2007. Doushantuo embryos preserved inside diapause egg cysts [J]. *Nature*, 446: 661–663.
- Yin Z, Zhu M, Davidson E H, et al. 2015. Sponge grade body fossil with cellular resolution dating 60 Myr before the Cambrian [J]. *Proceedings of the National Academy of Sciences of the United States of America*, 112(12): E1453–E1460.
- Yuan X, Chen Z, Xiao S, et al. 2011. An early Ediacaran assemblage of macroscopic and morphologically differentiated eukaryotes [J]. *Nature*, 470: 390–393.
- Zhang F, Frýda J, Fakraee M, et al. 2022. Marine anoxia as a trigger for the largest Phanerozoic positive carbon isotope excursion: Evidence from carbonate barium isotope record [J]. *Earth and Planetary Science Letters*, 584: 117421.
- Zhang Z, Zhou L, Chen X G, et al. 2024. Introduction of isotopically light barium from the Rainbow hydrothermal system into the deep Atlantic Ocean [J]. *Earth and Planetary Science Letters*, 625: 118476.